

**ENHANCING ASCE-41 MODELING GUIDELINES AND ACCEPTANCE CRITERIA  
USING INSTRUMENTED REINFORCED CONCRETE SHEAR WALL BUILDINGS**

Laura L. Hernández-Bassal and Sashi K. Kunnath

Department of Civil and Environmental Engineering  
University of California, Davis

**Abstract**

A preliminary set of evaluations on a low-rise reinforced concrete shear wall building is presented with the goal of assessing the modeling guidelines and acceptance criteria in ASCE-41 (ASCE/SEI 41, 2017). First, the ability of available commercial and open-source software to simulate the nonlinear flexural and combined shear-flexural response of experimentally tested walls is investigated. Next, a commonly-used commercial software, Perform-3D (CSI 2021) is utilized to conduct an assessment of a 3-story shear-wall building wherein all four analysis methods specified in ASCE-41 are applied. The simulation model is validated against instrumented data obtained during the 2010 Maricopa earthquake prior to its use in the ASCE-41 assessments. Results of the different assessments indicate that linear procedures are highly conservative with Collapse Prevention limits being exceeded whereas the application of nonlinear procedures suggest that the building performance is within Life Safety limits.

**Introduction**

Beyond facilitating the seismic assessment of buildings, the guidelines in ASCE-41 (ASCE/SEI 41, 2017) also represent a significant advance in the practice of performance-based earthquake engineering. However, calibration of the analysis procedures and acceptance criteria to real building performance should be a continuing effort. The use of strong motion data obtained from instrumented buildings experiencing strong ground shaking is an essential part of this process.

However, many of the nonlinear modeling guidelines in ASCE-41 include unspecified parameters left to the judgement of the engineer – with the potential for considerable variation in the predicted seismic demands. Additionally, as pointed out in a recent research report (NEHRP Consultants Joint Venture, 2013), “ASCE/SEI 41 generalized force-deformation curves are presented with single, deterministic values, without any information on the uncertainty or reliability of the parameters.” Another issue that arises from using ASCE-41 is the choice of the analysis procedure since as many as four are permitted to estimate seismic demands: Linear Static Procedure (LSP), Linear Dynamic Procedure (LDP), Nonlinear Static Procedure (NSP), and Nonlinear Dynamic Procedure (NDP). This implies that the assessment of a regular low to mid-rise building (that meets the criteria for the use of linear and/or static procedures) using any of the methods should result in the same conclusion on the likely performance of the building.

The aforementioned issues are being addressed in an ongoing project that focuses on modeling and acceptance criteria for shear-wall buildings. Shear wall buildings form an

important subset of RC buildings and are a common choice for buildings where deformation control is important. Since shear walls make up the primary (and generally the only) lateral force resisting system in a building, they are less redundant than moment-frame structures and damage or failure of a single wall can have more significant consequences on the performance of the structure.

### Assessment of Existing Shear Wall Models

ASCE-41 does not provide specific guidelines on modeling a shear wall element. Many options exist for modeling a concrete wall: the simplest approach is to model the wall as a beam-column element with inelastic behavior lumped into a concentrated spring with aggregated shear; the next level of refinement would be a beam-column element with distributed properties where selected integration points are discretized into fibers representing cover concrete, core concrete and reinforcing steel. RC walls have also been modeled using multi-spring macro-models consisting of a set of springs distributed in a manner that captures the strain distribution across the section of the wall as well as the migration of the neutral axis under lateral cyclic loading. In order to understand the capabilities of the available 2D models in different software programs, two computational platforms were considered: OpenSees (McKenna, 2011) and Perform-3D (CSI 2021). Validation studies were carried out on two shear wall specimens. The first wall considered is specimen **RW2** (Fig. 1a), part of the set of walls tested by Thomsen and Wallace (1995). This is a relatively slender wall with a height to width ratio of 3.0, in which inelastic deformations are expected to be dominated by flexure, and subjected to a constant axial load of  $0.07 f'_c A_g$  throughout the test. The second wall is specimen **RW-A15-P10-S78** (Fig. 1b), tested by Tran and Wallace (2012). This wall has a height to width ratio of 1.5 and nonlinear shear deformations are expected to contribute to the overall response. A constant axial load of  $0.064 f'_c A_g$  was maintained at the top of the wall. Both wall elevations are shown in Fig. 1.

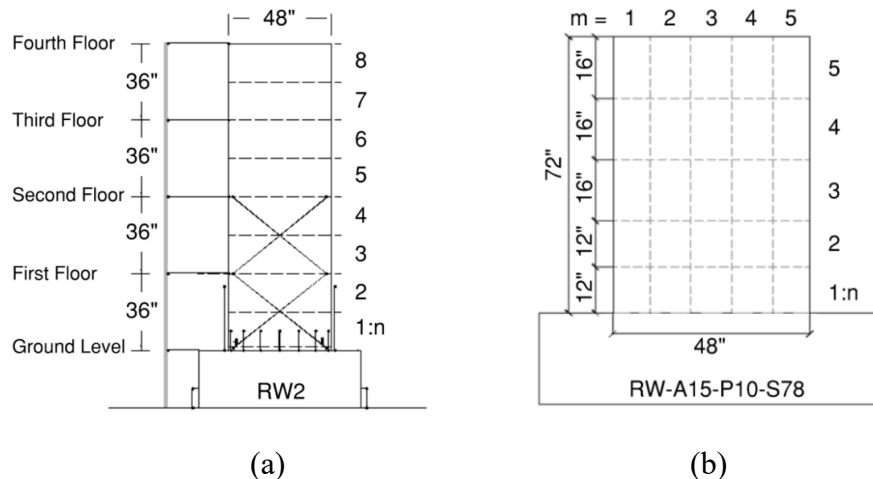


**Figure 1. Elevation of wall specimens: (a) Specimen 1 (Thomsen & Wallace 1995); (b) Specimen 2 (Tran & Wallace 2012)**

The two walls were modeled in OpenSees using three different modeling options: a beam-column element with fiber-section discretization, the Multiple Vertical Line Element

Model (MVLEM), and the Cyclic Shear-Flexural Interaction Multiple Vertical Line Element (SFI-MVLEM). They were modeled in Perform-3D using the Shear Wall element with Inelastic section – for Specimen 1, an elastic shear material was used whereas an inelastic shear material was used for Specimen 2. Note that MVLEM and SFI-MVLEM are derivatives of the original element introduced by Japanese researchers (Kabeyasawa et al. 1983) and later enhanced by others (Orakcal et al. 2004; Massone et al. 2006; Kolozvari et al. 2015).

Fig. 2 compares the numerically simulated response for Specimen 1 versus the measured cyclic response for all four modeling choices. In general, all models produce a good match. Both the MVLEM and SFI-MVLEM models capture the initial stiffness well, whereas the beam-column with fiber-section and Perform-3D models slightly overestimate it though they do a better job in predicting the strength in each cycle. Since the material models in Perform-3D are multilinear, the resulting force-deformation response is also multilinear.

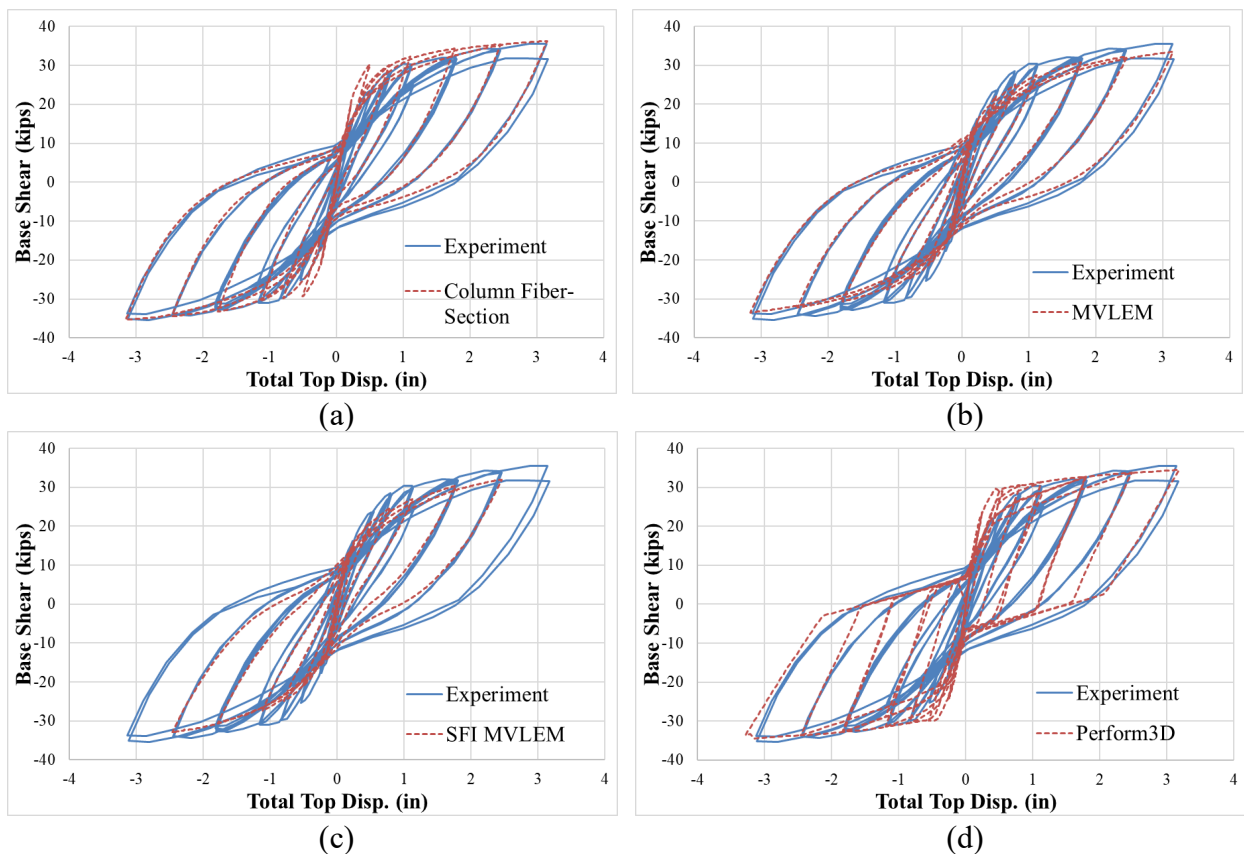


**Figure 2. Validation of modeling approaches using results from Specimen 1:**  
**(a) OpenSees with beam-column element and fiber section; (b) OpenSees MVLEM;**  
**(c) OpenSees SFI-MVLEM; (d) Perform-3D**

Fig. 3 shows the results for Specimen 2. It is evident that the SFI-MVLEM model produces the best results. The beam-column element with fiber-section (and aggregated shear spring) and the MVLEM model are unable to accurately capture the pinched response observed in the experiment. In Perform-3D, it is unclear as to how shear is coupled with flexure. The manual simply indicates that the shear wall is a “compound” element with either elastic or

inelastic shear material. Despite numerous attempts to tune the inelastic shear material properties, it was difficult to obtain a suitable response.

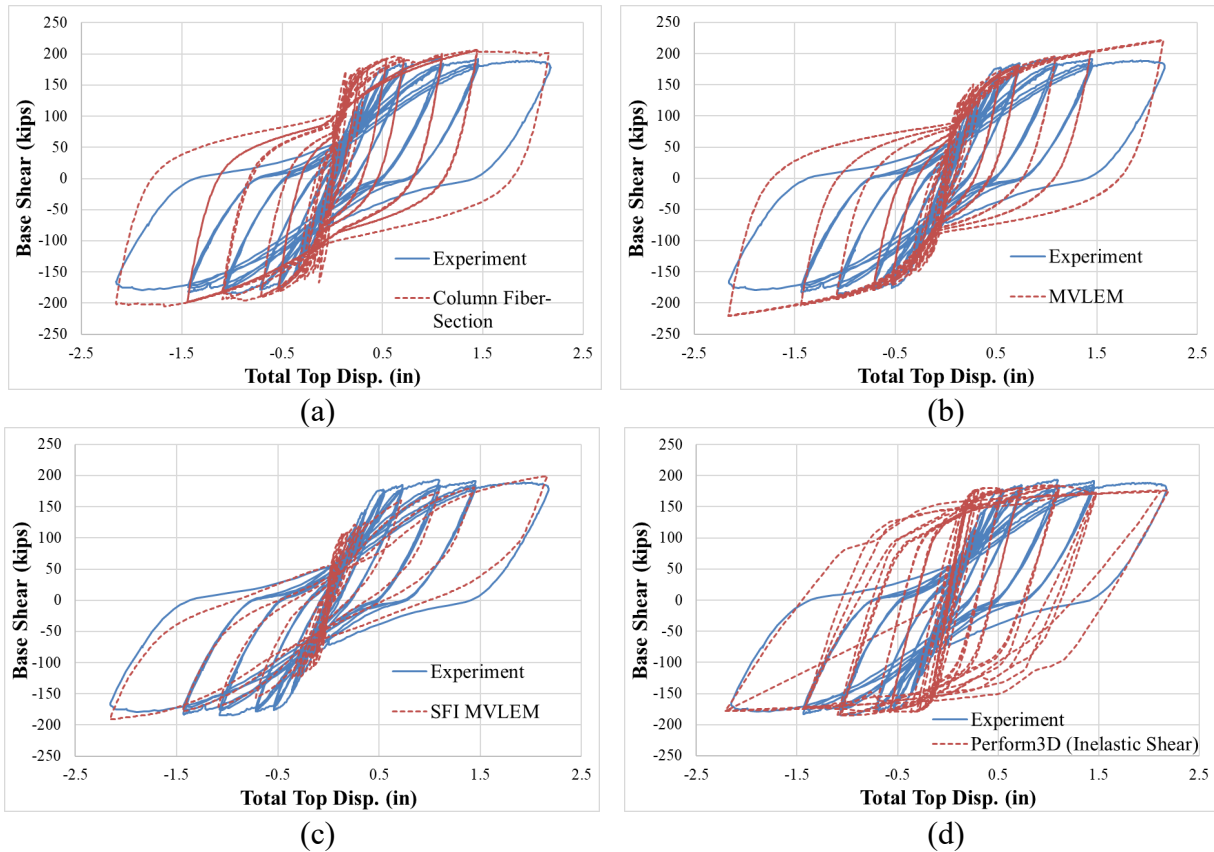


**Figure 3. Validation of modeling approaches using results from Specimen 2:**  
**(a) OpenSees with beam-column element and fiber section; (b) OpenSees MVLEM;**  
**(c) OpenSees SFI-MVLEM; (d) Perform-3D**

### Building Assessment: Modeling and Validation

In order to realistically evaluate the issues outlined in the introduction, it is important to begin with realistic computer models of existing buildings. Hence calibrating the models to observed data is a critical aspect of the proposed evaluation – since the contribution of non-structural components is inherent in the measurements. The first structure selected for the assessment is a 3-story school building designed in 1948 and located in Taft, California. The gravity system is composed of reinforced concrete slabs, supported on pan joists, and beams, supported by walls and columns. The lateral force resisting system includes concrete slab diaphragms and shear walls. There are four principal L-shaped walls at the corners with embedded columns at the gridlines, and two additional rectangular walls in the longitudinal direction. The building wall framing conserves symmetry. Fig. 4 shows the typical floor plan of the building.

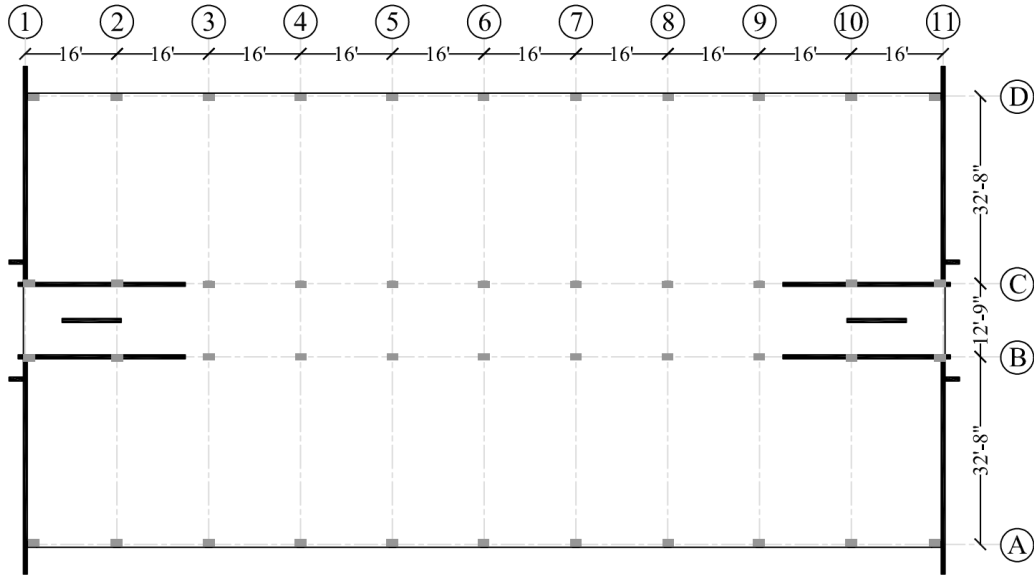


Figure 4. Plan view of building at typical floor

The building has been instrumented by the California Strong Motion Instrumentation Program (CSMIP Station 35409) with thirteen accelerometers: six at the ground level to record base accelerations in all three orthogonal directions, three at the 2<sup>nd</sup> floor, and four at the roof of the building – as shown in Fig. 5. There are a total of six recorded earthquakes measured at this site. However, only the 2010 Maricopa Earthquake sensor recordings will be used for the calibration since this is the earthquake with the largest ground peak acceleration.

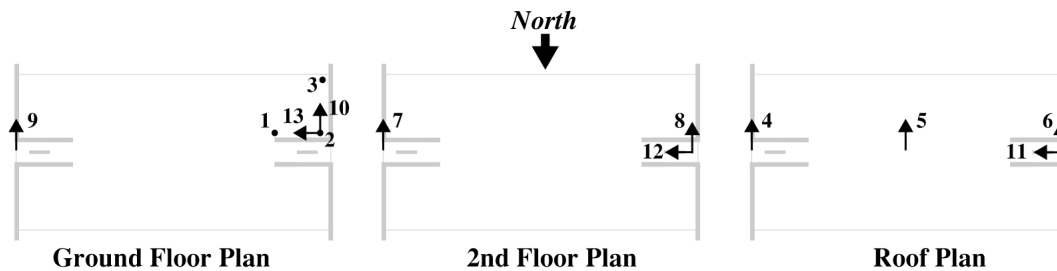
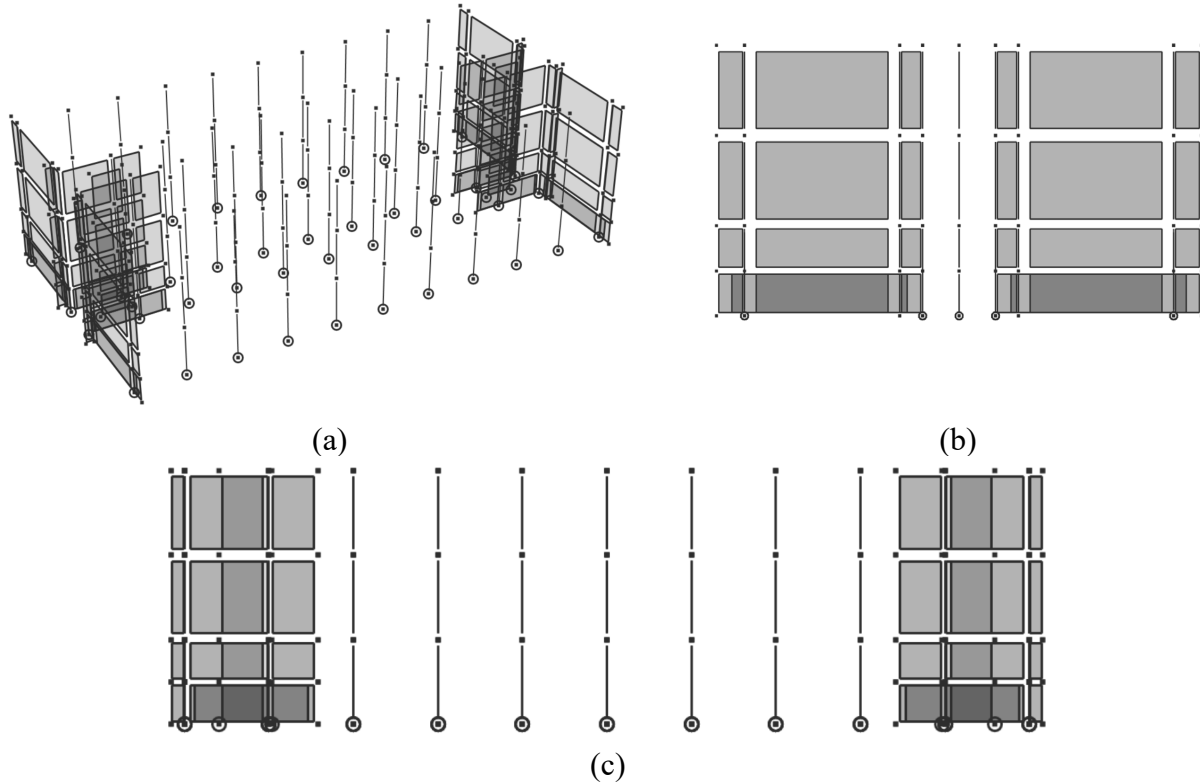


Figure 5. Locations of installed sensors

### Modeling and Validation

Given that the main lateral load resisting system is composed of L-shaped walls, it was necessary to create a three-dimensional building model, in order to capture any potential torsional modes as well as to account for non-symmetric response following inelastic action. Therefore, the analyses were carried out using the commercial software Perform-3D (CSI 2021). Fig. 6 shows the 3D and transverse/longitudinal elevation views of the model.



**Figure 6. Perform3D model: (a) 3D view, (b) N-S elevation (transverse), (c) E-W elevation (longitudinal)**

The walls were modeled using the *Shear Wall, Inelastic Section*, and the columns using the *Column, Inelastic Fiber Section*. The wall elements at the first story were divided into two elements along the height, to ensure a proper hinge length for inelastic action, while the upper story walls were modeled at the full height for each element. The unconfined and confined concrete were modeled using the *Inelastic 1D Concrete Material*, and were assigned to the walls and columns respectively. The rebar was modeled using the *Inelastic Steel Material, Non-Buckling*. For both concrete and steel materials, strength loss was considered. The parameters used follow the stress-strain relationship shown in Fig. 7 and are listed in Table 1. Cyclic degradation for the three materials was specified with the following energy factors: 1, 0.4, 0.4, 0.1, 0.1 at points Y, U, L, R, and X respectively, as recommended by Lowes et. al (2016). The shear material was specified as elastic with a shear modulus equal to 0.4 times the elastic modulus.

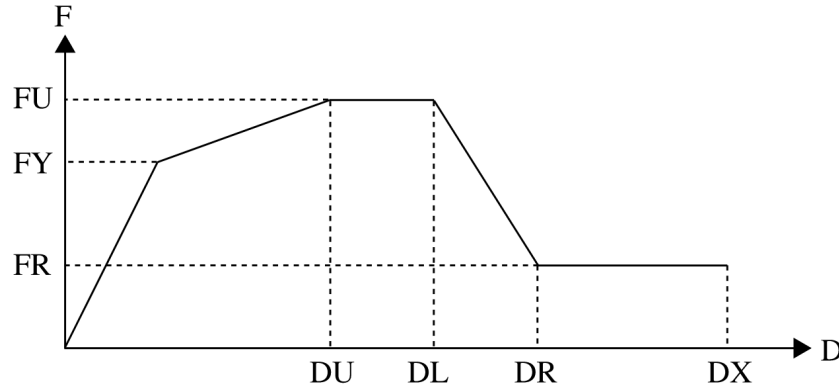
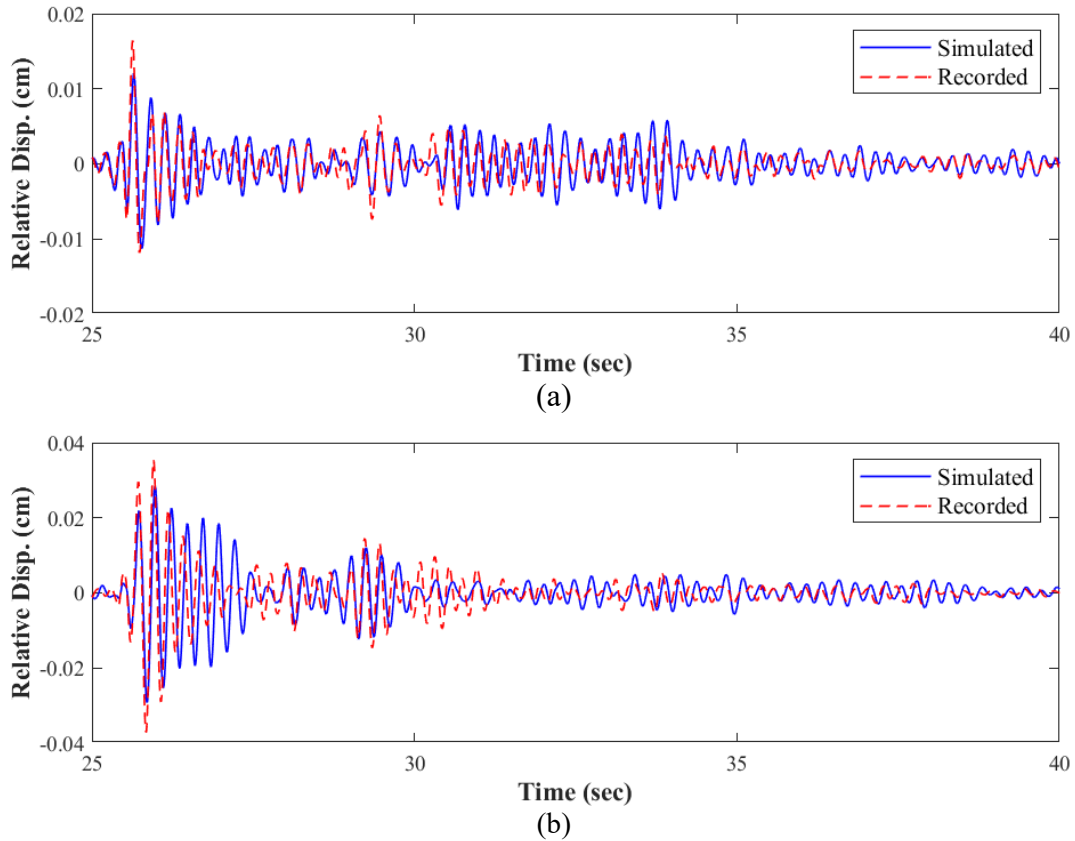


Figure 7. Perform-3D: Parameters for stress-strain relationships

Table 1. Stress-strain properties

Properties	Unconfined Concrete	Confined Concrete	Steel Rebar
E (ksi)	3491	3694	29000
FY (ksi)	2.25	2.52	41.25
FU (ksi)	3.75	4.2	51.5625
DU	0.0025	0.0035	0.045
DL	0.003	0.004	0.07
DR	0.01	0.035	0.1
DX	0.2	0.2	0.2
FR/FU	0.1	0.2	0.2

A diaphragm constraint was applied at each level. There are elastic springs at all base nodes which have a footing. The spring stiffness values were originally calculated and updated in the model; however, the analysis showed that the foundation was introducing too much flexibility to the system. Therefore large stiffness values were assigned to the springs, essentially creating a fixed base model, and better capturing the recorded response in the model. An eigenvalue analysis was carried out on the model and the first and second mode periods were estimated to be 0.194 sec and 0.143 sec in the longitudinal and transverse directions, respectively. A value of 7.5% of critical damping in the two modes were assigned. The structure was then subjected to the recorded base motion during the Maricopa earthquake. The corresponding ground motions recorded at sensors 13 and 10 were applied to the longitudinal and transverse directions, respectively. Fig. 8 compares the simulated and recorded roof response after final calibration of the model.



**Figure 8. Comparison of recorded vs. simulated roof displacement histories during the Maricopa earthquake: (a) Transverse; (b) Longitudinal direction**

### **Building Assessment using ASCE 41 Guidelines**

A seismic performance assessment of the building was carried out by analyzing the validated computer model of the 3D building and using both linear and nonlinear analysis procedures prescribed in ASCE 41. Note that in all procedures described hereafter, the lateral load application is preceded by the application of the sustained gravity loads on the frame. The seismicity considered in the assessment is based on the BSE-2E hazard level, which represents a 5% probability of occurrence in 50 years. The resulting response spectrum for the site is shown in Fig. 9 with the following key parameters:  $S_{XS} = 1.23$  g;  $S_{X1} = 0.873$  g;  $T_O = 0.14$  sec and  $T_S = 0.71$  sec.



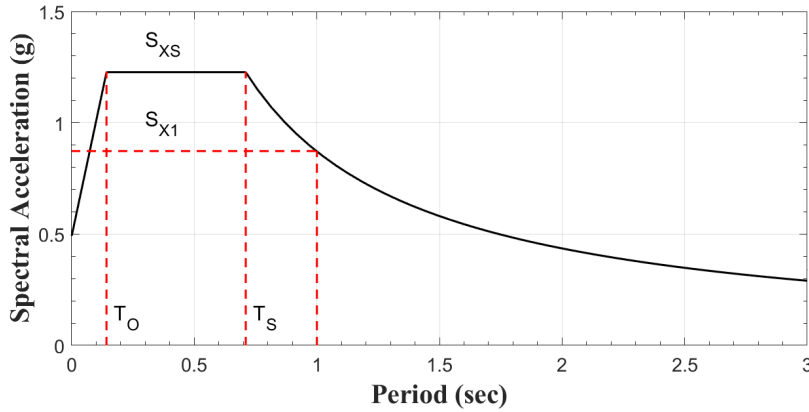


Figure 9. Response spectrum for site

### Linear Procedures

For the linear procedures, linear elastic materials were specified in Perform-3D. For the Linear Static Procedure (LSP), an equivalent static load, representative of the seismic hazard, is applied over the height of the building, in each horizontal direction independently. The modification factors are  $C_1C_2 = 1.0$  and  $C_m = 0.8$ . The effective seismic weight is 5858 kips for the full building. For the Linear Dynamic Procedure (LDP), the assessment was completed by using the Response Spectrum load case type in Perform3D, ensuring that the modes considered captured at least 90% of the participating mass of building. For both linear procedures, the demands in the components were obtained by applying the 100%-30% and 30%-100% combination rule. The walls in the building have been identified in Fig. 10. The final results for the linear procedures are listed in Table 2, and visually presented in Fig. 11. The LSP and LDP results are consistent, with two walls complying with Life Safety (LS), two walls complying with Collapse Prevention (CP), and six walls exceeding CP.

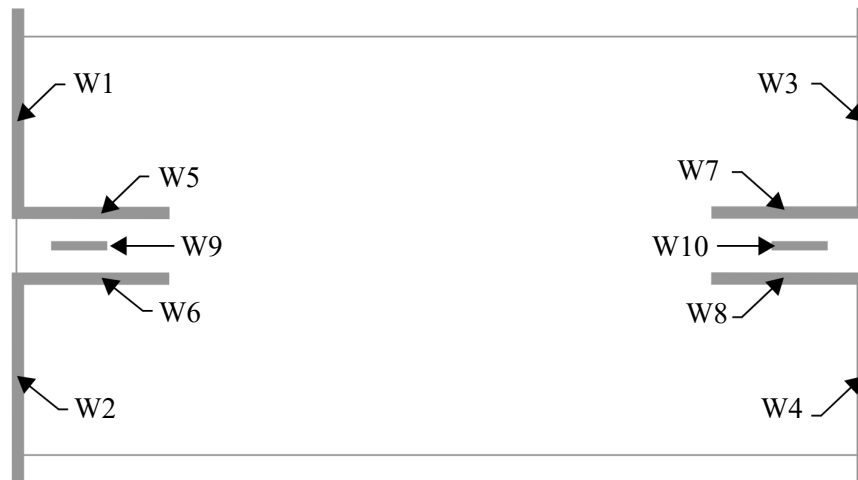
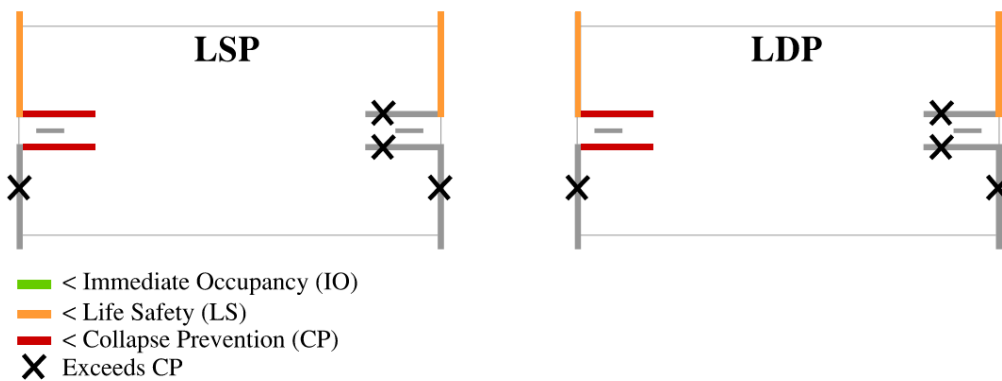


Figure 10. Plan view identifying wall elements

**Table 2: LSP and LDP results**

Wall #	Capacities	LSP Demands		LDP Demands		ASCE -41 m-Factors		
	V (k)	V (k)	DCR	V (k)	DCR	IO	LS	CP
W1	583	1411	2.4	1722	3.0	2	3	4
W2	229	1411	6.2	1722	7.5	2	3	4
W3	583	1411	2.4	1722	3.0	2	3	4
W4	229	1411	6.2	1722	7.5	2	3	4
W5	356	1229	3.5	1425	4.0	2	3	4
W6	356	1229	3.5	1425	4.0	2	3	4
W7	184	1229	6.7	1425	7.7	2	3	4
W8	184	1229	6.7	1425	7.7	2	3	4



**Figure 11. Results of LSP and LDP assessments**

### Nonlinear Procedures

For the nonlinear procedures, the original nonlinear model was used in the analyses. For the Nonlinear Static Procedure (NSP), the building was pushed to the computed target displacements of 7.16 in (0.0124 drift) and 4.10 in (0.0071 drift) in the longitudinal and transverse directions, respectively. The maximum demands obtained from the two analyses were used in the assessment of the building performance.

For the Nonlinear Dynamic Procedure (NDP), the site hazard was established using the United States Geological Survey (2018) Unified Hazard Tool, based on the site deaggregation. The seismic hazard at the site is controlled by the San Andreas fault. A total of 51 ground motions were downloaded from the PEER NGA ground motion database (ngawest2.berkeley.edu) with the following filters: fault type: strike slip; magnitude: 6 to 8; distance to rupture: 5 to 25; and shear wave velocity  $V_{s30}$ : 200 to 400 m/s, based on the controlling seismic hazard at the site. Ground motions with spectral shapes significantly different from the target spectrum were discarded. The final 11 sets of ground motion (pairs) were selected such that the average maximum direction spectra (RotD100) was at or above 90% of the target response spectrum in the period range  $0.2T_1 - 1.5T_1$ . Even though the site is classified as near-fault, the horizontal components of each selected ground motion were not rotated to the

fault-normal and fault-parallel directions of the causative fault. Fig. 12 shows the selected records spectral accelerations, and Table 3 lists the details of the ground motions.

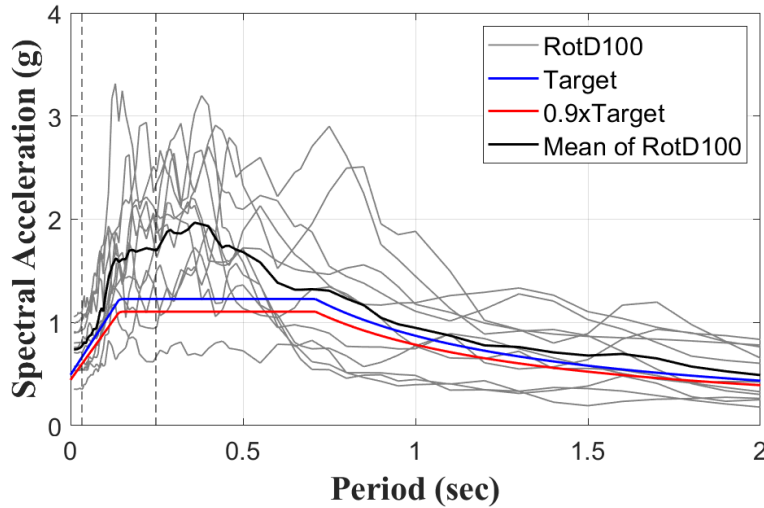


**Figure 12. Maximum direction spectra of scaled motions, mean spectra, and site target spectrum**

**Table 3: Selected ground motions**

GM #	Record Sequence Number	Earthquake Name	Year	Station Name	Magnitude	R <sub>rup</sub> (km)
1	30	"Parkfield"	1966	"Cholame - Shandon Array #5"	6.19	9.58
2	162	"Imperial Valley-06"	1979	"Calexico Fire Station"	6.53	10.45
3	169	"Imperial Valley-06"	1979	"Delta"	6.53	22.03
4	179	"Imperial Valley-06"	1979	"El Centro Array #4"	6.53	7.05
5	184	"Imperial Valley-06"	1979	"El Centro Differential Array"	6.53	5.09
6	185	"Imperial Valley-06"	1979	"Holtville Post Office"	6.53	7.5
7	558	"Chalfant Valley-02"	1986	"Zack Brothers Ranch"	6.19	7.58
8	1101	"Kobe_ Japan"	1995	"Amagasaki"	6.9	11.34
9	1107	"Kobe_ Japan"	1995	"Kakogawa"	6.9	22.5
10	1158	"Kocaeli_ Turkey"	1999	"Duzce"	7.51	15.37
11	1605	"Duzce_ Turkey"	1999	"Duzce"	7.14	6.58

For each ground motion set, the horizontal components were applied concurrently to the model, and then again applied but with the directions switched. The maximum demands for each set were calculated and then used to compute the average demands of the eleven ground motion sets. Table 4 lists the results for both nonlinear procedures and Fig. 13 shows the performance level compliance. The results show that all walls satisfy the LS criteria for NSP, and the IO criteria for NDP. This is significantly different than the performance levels satisfied by the linear procedures.

**Table 4: NSP and NDP results**

Wall #	NSP Max Rotation	NDP Max Rotation	ASCE 41 Acceptable Plastic Hinge Rotation		
			IO	LS	CP
W1	0.0127	0.0020	0.0050	0.0150	0.0150
W2	0.0130	0.0021	0.0050	0.0150	0.0150
W3	0.0127	0.0017	0.0050	0.0150	0.0150
W4	0.0130	0.0016	0.0050	0.0150	0.0150
W5	0.0067	0.0029	0.0050	0.0150	0.0150
W6	0.0067	0.0029	0.0050	0.0150	0.0150
W7	0.0069	0.0029	0.0050	0.0150	0.0150
W8	0.0069	0.0029	0.0050	0.0150	0.0150

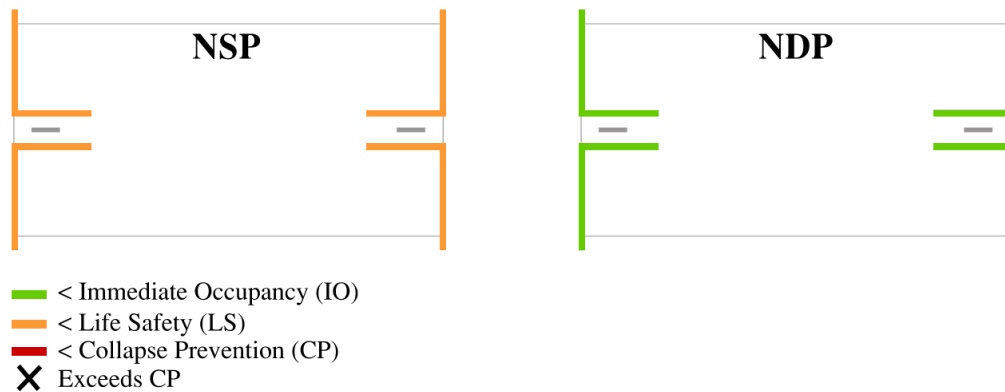


**Figure 13. Results of the assessments using NSP and NDP**

### Conclusions

A comparative study of modeling approaches was completed for two reinforced concrete wall specimens. The walls were modeled using a total of four distinct modeling schemes in OpenSees and Perform3D. The results show that for the flexure-controlled specimen, the MVLEM and SFI-MVLEM models in OpenSees better captured the initial stiffness and the OpenSees beam-column with fiber-section and Perform-3D shear wall models better predicted the strength, albeit all models produced a reasonable match of the overall cyclic force-deformation response. In the shear-controlled specimen, the SFI-MVLEM produced the best results, capturing the stiffness, strength and pinched response under cyclic loading.

An existing three-story shear wall concrete building was selected for the ASCE-41 based assessment. Given the L-shaped walls in the building, it was decided to use Perform-3D for the assessment since SFI-MVLEM was considered more suitable for planar walls. Following calibration of the model to instrumented response from a recent earthquake, a preliminary ASCE-41 assessment was completed utilizing both linear and both nonlinear analysis procedures. The results show that LSP and LDP produced demands exceeding the acceptance

criteria for the CP performance level for as many as four walls. However, the NSP and NDP demands satisfied LS and IO, respectively, for all walls. This demonstrates inconsistency among the four analysis procedures and is the subject of additional ongoing investigation.

### Acknowledgements

Funding for this study was provided by the California Department of Conservation, California Geological Survey (Strong Motion Instrumentation Program) under Agreement 1020-005. However, the contents of the paper do not necessarily represent the policy of that agency nor is an endorsement by the State Government of California.

### References

- ASCE/SEI (2017). *Seismic Evaluation and Retrofit of Existing Buildings*, ASCE/SEI 41-17, American Society of Civil Engineers, Reston, Virginia.
- CSI (2021). *Perform-3D: Performance-Based Design of 3D Structures*. Computers and Structures Inc., Walnut Creek, CA.
- Kabeyasawa, T., Shiohara, H., Otani, S. and Aoyama H. (1983). Analysis of the full-scale seven-story reinforced concrete test structure. *J. Fac. Eng., University of Tokyo*.XXXVII:2,432–78.
- Kolozvari K., Orakcal K., and Wallace J. W. (2015). "Modeling of Cyclic Shear-Flexure Interaction in Reinforced Concrete Structural Walls. I: Theory", *ASCE Journal of Structural Engineering*, 141(5).
- Lowes, L., Lehman D., and Baker, C. (2018). *Recommendations for Modeling the Nonlinear Response of Slender Reinforced Concrete Walls Using PERFORM-3D*, 2016 SEAOC Convention Proceedings, 2016.
- Massone, L.M., Orakcal, K. and Wallace J.W. (2006). Shear–flexure interaction for structural walls. *ACI special publication—Deformation capacity and shear strength of reinforced concrete members under cyclic loading*. ACI-SP236-07, 127–150.
- McKenna, F. (2011). *OpenSees: a framework for earthquake engineering simulation*. *Computational Science & Engineering*, 13 (4), 58-66. <https://doi.org/10.1109/MCSE.2011.66>
- NEHRP Consultants Joint Venture (2013). "Nonlinear Analysis Research and Development Program for Performance-Based Seismic Engineering," NIST GCR 14-917-27, National Institute of Standard and Technology, US Department of Commerce, Gaithersburg, MD.
- Orakcal, K., Wallace, J.W., and Conte, J.P. (2004). Flexural modeling of reinforced concrete walls—model attributes. *ACI Structural Journal*.101:5,688–98.

Thomsen, J. H., IV, and Wallace, J. W. (1995) “Displacement-based design of reinforced concrete structural walls: Experimental studies of walls with rectangular and T-shaped cross sections.” Rep. No. CU/CEE-95/06, Department of Civil and Environmental Engineering, Clarkson University, Potsdam, NY.

Tran T.A. and Wallace J.W. (2012). Experimental study of nonlinear flexural and shear deformations of reinforced concrete structural walls, Proceedings, 15th World Conference on Earthquake Engineering, Lisbon, Portugal.